

Article

Laser Processing of Liquid Crystal Droplets with Diverse Internal Structures

Jin-Kun Guo ^{1,*} , Jinzhong Ling ¹, Ying Yuan ¹, Fengjiao Chang ², Xiaorui Wang ^{1,*} and Jang-Kun Song ^{3,*}¹ School of Optoelectronic Engineering, Xidian University, Xi'an 710071, China² South Campus, Shaanxi University of Chinese Medicine, Xianyang 712046, China³ School of Electronic and Electrical Engineering, Sungkyunkwan University, Suwon 440-746, Gyeonggi-do, Republic of Korea

* Correspondence: jkguo@xidian.edu.cn (J.-K.G.); xrwang@mail.xidian.edu.cn (X.W.); jk.song@skku.edu (J.-K.S.)

Abstract: To control the spatial placement and organize micro/nanodroplets (NDs) has fundamental importance both in science and engineering. Cholesteric liquid crystal (CLC) droplets with topological diversity can offer many self-assembly modalities to arrange guest NDs in their spherical confinement; however, limited progress has been achieved due to difficulties of loading NDs into stabilized host droplets. Here, a laser injection technique is introduced, through which a controlled number of NDs were injected from a pre-selected location onto the surface of the host droplet. The sequentially injected NDs spontaneously drifted toward areas with topological defects and self-assembled along its geometry or local director field into a predefined shape. Within CLC droplets with different topological structures, guest NDs self-assembled near areas with defect points as twisting radial chains and quill-like assembly structures, and along defect lines as discrete beads and helical threads, respectively. The injection speed of the NDs, controlled by laser power, was found to play a key role in the assembly geometry of NDs as well as the internal structure of the CLC droplet processed. This study expands our abilities to precisely organize NDs in a spherical confinement and such droplet-based microsystems have potential applications for sensors, photonic devices, pharmaceuticals, and biotechnology.

Keywords: liquid crystal; droplet; laser micro/nano manufacturing; laser injection; double emulsions; self-assembly; colloids; topological defect; templated self-assembly; colloidal liquid crystals



Citation: Guo, J.-K.; Ling, J.; Yuan, Y.; Chang, F.; Wang, X.; Song, J.-K. Laser Processing of Liquid Crystal Droplets with Diverse Internal Structures.

Crystals **2023**, *13*, 683. <https://doi.org/10.3390/cryst13040683>

Academic Editor: Borislav Angelov

Received: 20 March 2023

Revised: 6 April 2023

Accepted: 14 April 2023

Published: 16 April 2023



Copyright: © 2023 by the authors. Licensee MDPI, Basel, Switzerland. This article is an open access article distributed under the terms and conditions of the Creative Commons Attribution (CC BY) license (<https://creativecommons.org/licenses/by/4.0/>).

1. Introduction

The programmable arrangement of micro- or nanodroplets (NDs) into a designed structure with specific functions has attracted significant attention in both science and engineering [1–6]. It can be exploited in areas such as miniature photonic devices [7–9], intelligent sensors [10], functional microcapsules [11], artificial cells [12], and in vitro diagnostics [13–15]. With the help of material elasticity, liquid crystals (LCs) are ideal media to guide the NDs to self-assemble into predefined structures such as parallel ribbons [16], self-connected microwires [17], necklace rings [18], helicoidal threads [19], and hexagonal arrays [20]. The arrangement of NDs can be further manipulated by tuning the alignment of LC molecules with external stimuli such as electric fields [21,22], magnetic fields [3], and temperature [23], which further facilitates its application.

In the case of cholesteric LC (CLC) droplets, their topological diversity has been extensively reported [24,25], indicating their enormous potential as novel modalities for the templated self-assembly and positioning of NDs in three dimensions (3D). However, there are technical difficulties that hinder their development. First, by using a conventional top-down method such as a microfluidic droplet generator, it takes hours or even days to stabilize the topological structure of CLC droplets after emulsification. Before that, the organization of guest NDs in the host CLC sphere is beyond control and, in most

cases, NDs will aggregate into irregular-shaped clusters that are normally irreversible [3]. Second, the key to arranging NDs into an organized structure in an LC medium is to control their self-assembly dynamics using an optical tweezer. However, due to their spherical confinement, this method no longer works. Third, once the CLC-ND mixture is dispersed in a solution, there is no effective method to further vary the concentration of NDs in the isolated CLC droplets. However, to complement the assembly of NDs with sophisticated structures, the ability to successively send a certain number of NDs to a pre-selected location is indispensable.

In this work, we applied the laser-induced ND injection technique, as reported in our previous studies [18,26,27], to process cholesteric LC droplets with diverse internal structures. CLC droplets with various topological structures, defect points, or lines were prepared as the hosts by varying the chirality and surface anchoring. As the CLC droplets were prepared using pure CLC, their topological structure was well-established without the intervention of NDs. By manipulating the laser beam, water NDs were injected into the stabilized CLC droplet at a pre-selected surface location with a controllable size and number. The sequentially injected NDs self-assembled within the host CLC droplet into tailored structures such as twisting radial chains, quill-like structures, discrete beads, and helicoidal threads, respectively. Interestingly, apart from the self-assembly modality, we observed that changes in laser power could also control the geometric structure of the droplet being processed.

2. Materials and Methods

BHR20400 (liquid crystal) and R811 (chiral dopant) were purchased from Bayi Space, China. Sodium dodecyl sulfate (SDS, surfactant) and coumarin-6 (fluorescence dye) were purchased from Sigma-Aldrich. The water used in our experiments was purified using a Milli-Q water purification system (HHitech, Shanghai, China). The purchased chemicals were used as received without further modification or purification.

The CLC droplet preparation was as follows. The CLC material in different chiralities was mixed with BHR20400 and R811 with different doping concentrations based on a purpose. To homogeneously composite the mixture, it was sonicated for 0.5 h and stirred for 10 h. The CLC mixture was emulsified in an aqueous surfactant solution into droplets with a size in a range of 50 μm to 200 μm . The CLC emulsion was injected into a sandwiched glass cell for the experiment. To prevent water evaporation and maintain a constant surfactant concentration during laser processing, the cell was sealed by glue.

The microscopic analysis was performed using an inverted optical microscope (Ti2-U, Nikon, Shin-oyoke, Japan) with or without crossed polarizers. The pictures were captured by one CCD camera (TrueChrome AF, Tucsen, Xiamen, China), mounted on an eyepiece of the microscope.

For the fluorescence confocal polarizing microscopy (FCPM), a laser-scanning-type FCPM (K1-Fluo, Nanoscope systems, Seoul, Korea) was used to obtain horizontal sectional images at different vertical locations to detect the arrangement of NDs in the host CLC droplet [28]. To generate a fluorescence signal, coumarin-6 was doped into the CLC material at a ratio of 0.01 wt%. The pinhole was set to 1 a.u. and a 405 nm laser beam was used. Objectives with magnitudes of $\times 20$ and $\times 40$ and numerical apertures of 0.5 and 0.75 were used, respectively.

The laser injection and loading of the NDs were performed as follows. The optical setup of the laser processing system is illustrated in Figure 1. One 445 nm diode laser (LL-LASER, Changchun, China) was focused through the objective with $NA = 0.6$ (Nikon, Japan) and irradiated on the surface of the CLC droplets. The beam collimator (LBTEK, Changsha, China), beam expander (Thorlabs, Newton, NJ, USA), half-wave plate (LBTEK, Changsha, China), and polarizer (LBTEK, Changsha, China) were inserted into the light path in successive steps to shape the processing laser beam and control the laser power. The laser spot size was changed to 5 μm with power in a range of 0.1 mW to 0.8 mW. To

enhance the laser absorption and increase the laser-induced heating, 0.1 wt% of coumarin-6 was added to the targeted CLC droplets.

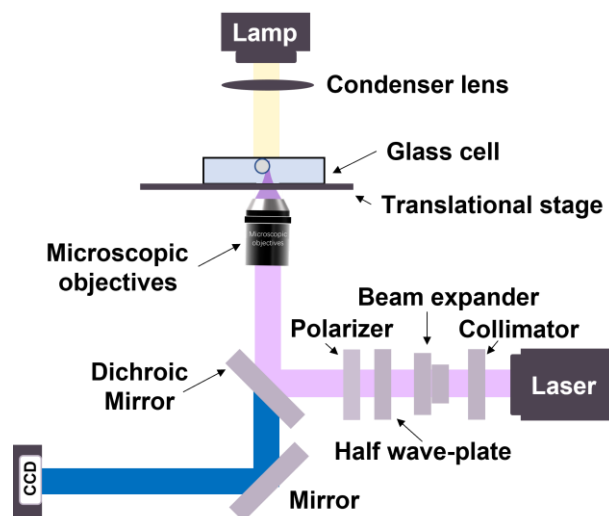


Figure 1. Schematics for the experimental setup.

3. Results

3.1. Injection of NDs into a Stabilized CLC Droplet by Laser

After the CLC mixture was emulsified into droplets and dispersed in an aqueous solution of surfactant (SDS), it underwent a relaxation process to reach an equilibrium, during which the molecular alignment of the LC within its spherical confinement was minimized in terms of energy [18,29]. For the thermotropic LC utilized in this study, this relaxation process typically lasted from a few to several tens of minutes, depending on the specific chemical composition. Once the relaxation process was complete, the topological structure of the CLC droplet was stabilized. This structure was determined by the droplet's chirality (N) and surface anchoring. The chirality of the droplet was dependent on the pitch (P) of the CLC mixture, which was linearly proportional to the concentration of the chiral dopant as well as the size of the CLC droplet (D), where $N = 2D/P$ [24,29]. Additionally, the SDS surfactant in the solution induced a perpendicular anchoring of the LC molecules to the surface of the CLC droplets [30]. However, by diluting the SDS concentration to below 0.01 mM, the surface anchoring could be changed to planar.

As illustrated by the schematic in Figure 1, the laser-induced ND injection technique was applied to load the guest NDs into the target CLC droplet with a stabilized topological structure. In brief, by directing a continuous laser beam at a pre-selected location on the surface of an LC droplet, this technique allowed the injection of a tiny amount of surrounding water solution into the LC droplet. With the help of the elasticity of LC molecules, the injected water solution spontaneously formed into monodispersed guest water NDs, which subsequently arranged themselves into a colloidal assembly within the host CLC droplet. In this way, it offered a bottom-up approach to assembling the internal structure of a mesoscale LC droplet [26].

3.2. Laser Processing of Cholesteric LC Droplets with Defect Points

For the CLC droplets with small chirality ($N < 6$), their topological structure was characterized by defect points that could be distinguished under crossed-linear polarizers. Within a CLC droplet, the region with defect points normally has the maximum splay energy, which can offer an attractive elastic force to the guest NDs [26]. In addition, the typical size of a defect point in thermotropic LCs is only 10 nm [31]. As a result, injected water NDs, which are on the micrometer scale, will self-assemble in the region with the defect point and arrange themselves along the local director field of a CLC droplet to minimize the free energy.

For the CLC droplet with $N = 2.3$ as the processing target, it contained a surface defect point (Figure 2). We irradiated the top surface of the CLC droplet with a $65 \mu\text{W}$ laser beam for 20 seconds at a time. For each exposure, a certain number of water NDs were injected into the CLC droplet and spontaneously drifted toward the area with the defect point. As illustrated in the time-sequenced images in Figure 2, the first-arrived ND was captured by the defect point (red dotted circle) and acted as the geometric center, whilst the other NDs were attached to it and successively aggregated into a twisting radial chain assembly. As more NDs joined, the sub-chains were lengthened and the whole assembly retracted from the surface toward the bulk of the host CLC droplet. To clarify its geometry in three dimensions (3D), we scanned the ND assembly using a confocal microscope and reconstructed its distribution (Figure 3). It is illustrated that all sub-chains were twisted and the hedgehog defect (red dot circle) stayed away from the boundary of the host sphere.

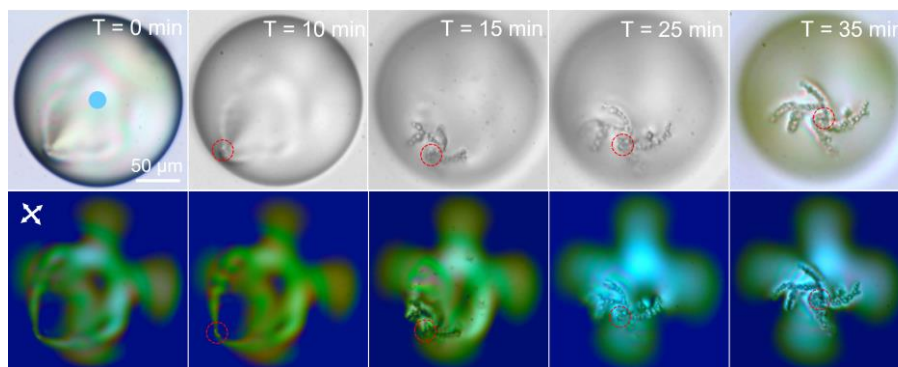


Figure 2. Laser processing of a CLC droplet with an internal structure of twisted radial chains. Laser irradiated ($65 \mu\text{W}$, 20 s, blue dot) the target CLC droplet and loaded guest water NDs into it. Time-sequenced microscopic images for the self-assembly of injected NDs into the CLC droplet with and without crossed-linear polarizers (white arrows).

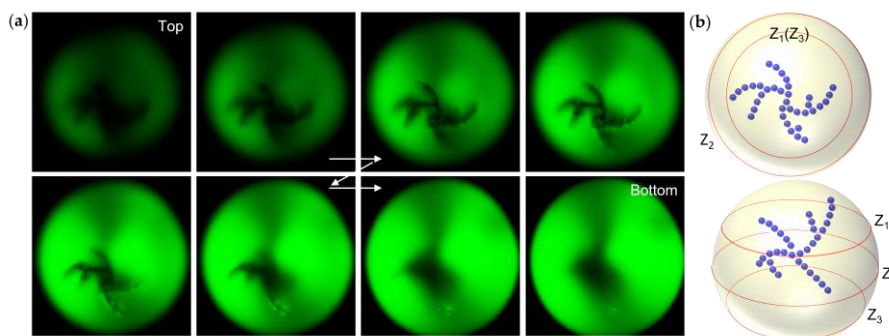


Figure 3. The geometry of the laser-processed CLC droplet in Figure 2. (a) Using a confocal microscope, the sequenced images illustrate the geometry of the CLC droplet in each vertical section; (b) 3D reconstruction of the distribution of ND assembly within the host CLC droplet.

Interestingly, we found that the NDs could also organize into a quill-like structure in the host CLC droplet with a single defect point. A CLC droplet with $N = 3.5$ was selected as the target for laser processing. In the beginning, it was difficult to distinguish its defect point, except for two bright strips visible under the microscope (red box in Figure 4a). A stronger laser irradiation ($127 \mu\text{W}$, 20 s) was then applied to the top surface of the CLC droplet. With the trapping of the first-injected ND, the location of the defect point was confirmed (red dotted circle). In addition, a stronger laser irradiation resulted in a faster injection speed. As a result, for each injection, the injected NDs gathered together and organized themselves into small curved chains (blue box in Figure 4b) near the irradiating area before drifting toward the defect area.

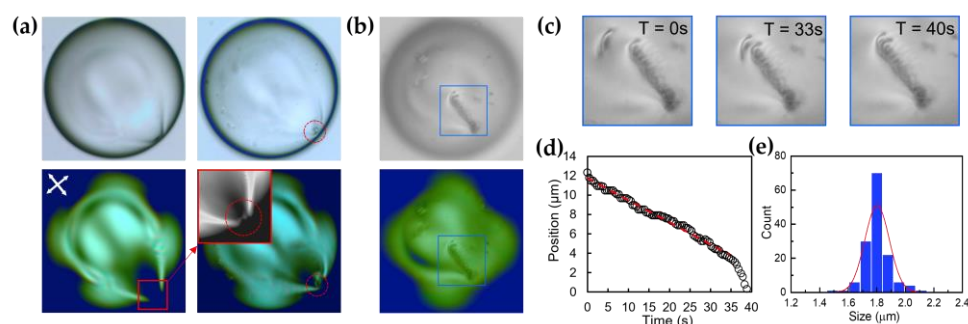


Figure 4. Laser processing of a CLC droplet with an internal quill-like structure. (a) Laser irradiated ($127 \mu\text{W}$, 20 s) the target CLC droplet with $N = 3.5$ and loaded guest water NDs into it. (b,c) For each irradiation, the injected NDs were organized into a curved chain and self-assembled as a single unit. (d) Time-sequenced position of curved chains for their self-assembly dynamics. (e) Size distribution of NDs in (b).

Remarkably, these pre-formed linear chains exhibited self-assembly as independent units (Figure 4b,c). One curved chain was attracted and drifted toward the ND assembly. During this process, this chain was always oriented parallel with the most outer one. When it moved closer, one droplet on this chain, prior to the rest, unexpectedly quickly attached to the most outer one. However, the rest would no longer approach further to their counterpart. In addition, the connections among these attached droplets, located on different curved chains, were relatively strong, which bonded different curved chains together. For the rest of the chains, or what we called the different branches, their connections were so weak that several of them could freely swing within a certain range. As more curved chains joined, a quill-like geometry was shaped near the surface area of the CLC droplet (blue box in Figure 4b). The dynamics are illustrated in Figure 4c,d, where each pre-formed chain drifted with a constant velocity ($T = 0\text{--}33$ s) and then accelerated to attach to the former trapped one ($T = 33\text{--}40$ s). With the help of ImageJ, the size distribution of the NDs was roughly estimated (Figure 4e). By adjusting the focal plane of the microscope, we found that the quill-like ND assembly spread out in opposite orientations near the top and bottom surfaces of the host CLC droplet, respectively (Figure 5).

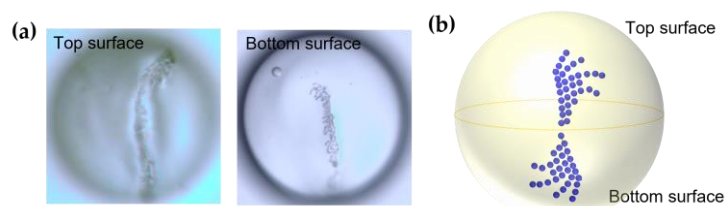


Figure 5. The geometry of the laser-processed CLC droplet in Figure 4. (a) By adjusting the focus of the microscope, a quill-like ND assembly near the top and bottom surface of the CLC droplets was observed. (b) The schematic drawing for the distribution in the host CLC droplet.

To exclude the effect of doping concentration to drive the difference in the assembly structure of the NDs for the two cases above, we selected a target CLC droplet with $N = 6$, which contained three defect points distributed on its symmetry axis (see Figure 6a). We then irradiated the laser at the surface areas of the CLC droplet near the defect points with a laser power of $65 \mu\text{W}$ and $127 \mu\text{W}$, respectively. By manipulating the loading speed of the NDs, the injected NDs were organized into two different assemblies: twisting radial chains, and quill-like structures, respectively (red boxes, Figure 6b). This demonstrated that, apart from the director field, the laser injection speed controlled by laser irradiation energy also played a key role in assembling the CLC droplet structure in 3D. In addition, by irradiating the top surface of the CLC droplet, the injected NDs were arranged into one straight linear chain along the symmetry axis of the host CLC droplet (Figure 6b).

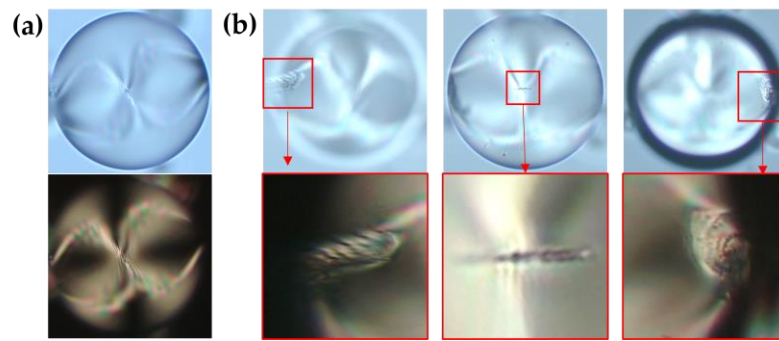


Figure 6. The impact of laser power on structural processing. (a) The CLC droplet with $N = 6$ contained three defect points. (b) Under laser irradiation, the injected water NDs self-assembled in the region with the defect point and arranged, along with the local director field, within the host CLC droplet. By adjusting the laser power, the injected NDs were organized into two different assemblies: twisting radial chains ($65 \mu\text{W}$) and quill-like structures ($127 \mu\text{W}$).

3.3. Laser Processing of Cholesteric LC Droplets with Defect Lines

The CLCs with large chirality ($N > 6$) exhibited a fingerprint texture, characterized by a topological defect line under planar surface anchoring. The defect line provided a large trapping potential for the NDs in the order of $1000 K_B T$, allowing them to stably stick onto it and self-assemble along its geometry [21,32]. Due to the high doping concentration of the chiral dopant in the LC medium, the LC molecules tended to form a layered helical structure that competed with their spherical boundary. The axis perpendicular to this helical layer was called the helical axis, as indicated by the 3D arrow in Figure 7 [18].

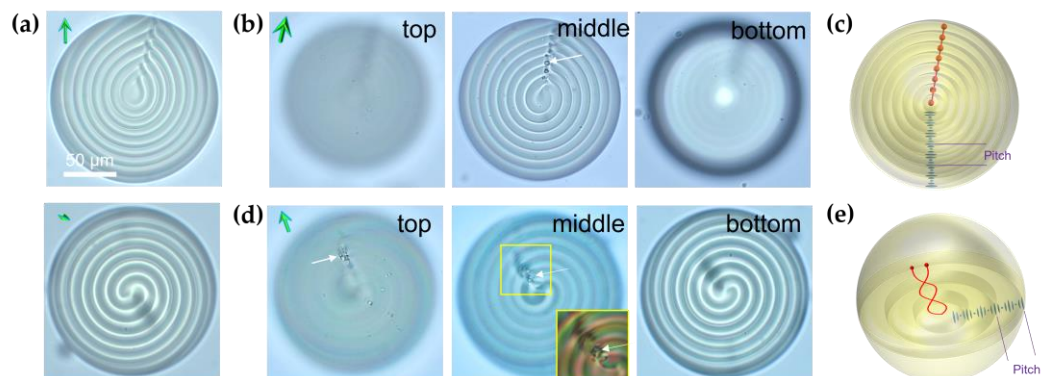


Figure 7. Laser processing of a CLC droplet with bulk defect line. (a) The microscopic texture of CLC droplets with $N = 15.6$. With different orientations of the helical axis (green axis in 3D), it changed from nesting cups (up image) to a double spiral (bottom image). (b,d) The injected NDs organized into two different assemblies in the host CLC droplet with the same chirality. The three images correspond with different focal planes of the microscope. (c,e) Schematics for the geometry of bulk defect line based on the structure of the ND assembly in (b,d), respectively. The 3D green arrow indicates the helical axis of the CLC droplet.

In the case of the target CLC droplets with $N = 15.6$, they involved defect lines forming a double helix structure that originated from the sphere center and terminated with two surface defect points. When observed under the microscope with or without a crossed-linear polarizer, the defect line could be distinguished as bright helical twisting strips with the aid of scattered light. Once the helical axis of the CLC droplets tilted out of the horizontal plane, its texture transformed from nesting cups into a double spiral (Figure 7a). Due to the tiny scale and delicate structure of the defect line, a precision laser injection is more demanding. Therefore, we tightly focused the light beam to less than $5 \mu\text{m}$ and irradiated the laser ($80 \mu\text{W}$, 5s) on the surface area of the CLC droplet near the region

with the defect line. To increase the quantity of injected NDs and, in the meantime, to avoid unwanted aggregation, we frequently adjusted the injection location through the laser-exposed area on the host microdroplet, but with the same input energy.

Interestingly, we observed that the injected NDs were organized into two different assembly structures in the CLC droplets with the same chirality. In the majority of cases, the injected water NDs assembled along the core of the defect line (black line) and merged into larger and discrete beads (white arrow and red beads), with an interval distance equal to half of the pitch (P) in the host CLC droplet, as illustrated in Figure 7b. In the minority of cases, the water NDs aligned along the geometry of the defect line to form a double helical droplet chain (Figure 7d; Supplementary Videos S1 and S2). By adjusting the focal plane of the microscope, the distribution of NDs in the CLC droplets of the above two cases and the geometry of the defect line were reconstructed in schematic drawings, as shown in Figure 7c,e.

4. Discussion

The laser injection technique introduces the concept of laser micro- and nanomanufacturing to the field of soft matter. By injecting water NDs into a stabilized LC droplet using a laser beam and controlling the self-assembly of the NDs into a predetermined internal structure of the host sphere, this technique offers a bottom-up approach to the assembly of three-dimensional droplet structures. Due to its non-contact and in situ processing characteristics, it enjoys a high degree of processing freedom. In this study, a laser system with an improved ability to manipulate the laser light was applied for the processing. We discovered that the laser power could also serve as a control parameter to influence the droplet structure being processed. Specifically, the laser power directly controlled the injection speed of water NDs into their host LC droplet. Before being attracted to the defect structure, all injected NDs near the irradiation area self-organized and joined the lateral assembly dynamics as a single unit. Therefore, changes in laser power not only simply impacted the injection number of NPs, but also contributed to the geometry of the assembly.

Cholesteric LC droplets with varying chirality and anchoring were used as the hosts to organize the NDs into diverse assemblies. The topological structure of the cholesteric LC host was well-established without intervention and the injected NDs spontaneously self-assembled and aligned along the director field or along the geometry of the defect line to minimize the free energy, which meant that the NDs could also act as a tracer to visualize the topological structure of their host.

Specifically, we observed that for CLC droplets with chirality of $N < 2$, the director field resembled that of the pure nematic case, with a radial configuration and one central defect point. As the chirality increased ($N = 2.3$), the central defect point moved toward the surface of the host sphere. However, the experimental data revealed that the director field remained unchanged and NDs continued to arrange into radial chains. At a certain value of chirality, the director field in the host sphere changed to a twisted radial configuration, as shown in Figure 2. This result was in good agreement with previous theoretical studies, which suggested that an increase in chirality leads to a decreasing twist elastic constant (K_{22}), eventually developing a non-zero azimuthal component and leading to a twisted radial configuration [33–35]. In addition, we observed that for CLC droplets with high chirality ($N > 6$) under planar anchoring, the NDs assembled into two different assembly structures; discrete beads in the majority case, and double helical droplet chains in the minority case. Even though it was impossible to distinguish the differences in the defect lines in these CLC droplets under an optical microscope, the assembly of the NDs demonstrated that the defect line had two distinct geometries. This result was consistent with the study of self-assembly in a lyotropic LC, which explained that a CLC droplet involves either one χ^{+2} defect line or two χ^{+1} defect lines [19]. In addition, the laser processing of CLC droplets with surface defect rings has been studied in our previous work [18].

In conclusion, combined with the non-contact and in situ processing capability of the laser injection technique and the abundant modalities offered by CLC droplets, we

processed the spherical structure of LC droplets with diverse internal structures. Compared with relying entirely on material self-assembly to process spherical structures, the laser injection method removed the restrictions of particle size as well as the boundary confinements, providing greater control over the self-assembly dynamics and making templated self-assembly a more versatile processing approach. This expands the design spectrum of architectures of soft materials, paves the way for the tailored assembling of the spherical structure of droplets, and could contribute to cutting-edge application development in the field of soft matter and complex liquid systems. In addition, the macroscopic properties of a droplet-based microsystem depend on its mesoscopic structure as well as its chemical composition. By injecting a solution together with active ingredients into the host CLC droplet, both the organization and chemical composition of the NDs within the host 3D space could be customized to perform a specific physical function. As a closed system, the internal structures of each droplet could be individually switched by tuning the orientation of the LC molecules with external stimuli such as electric fields and magnetic fields, which further facilitates the applications. Therefore, this could open a new path for the development of potential applications of droplet-based microsystems.

Supplementary Materials: The following supporting information can be downloaded at: <https://www.mdpi.com/article/10.3390/cryst13040683/s1>, Video S1: defect line geometry under cross-polarized optical microscope; Video S2: defect line geometry under optical microscope.

Author Contributions: Conceptualization, J.-K.G.; methodology, J.-K.G.; validation, J.L., Y.Y., F.C. and X.W.; formal analysis, J.-K.G.; investigation, J.-K.G.; resources, J.-K.G., X.W. and J.-K.S.; data curation, J.-K.G.; writing—original draft preparation, J.-K.G., J.L., Y.Y., F.C., X.W. and J.-K.S.; writing—review and editing, J.-K.G., X.W. and J.-K.S.; supervision, J.-K.G., X.W. and J.-K.S.; project administration, J.-K.G.; funding acquisition, J.-K.G., X.W. and J.-K.S. All authors have read and agreed to the published version of the manuscript.

Funding: This research was funded by the National Natural Science Foundation of China (NSFC 62005206, 62075176, and 62005204); the Key Research and Development Program of Shaanxi (2023-YBGY-003); The Fundamental Research Funds for the Central Universities (ZYTS23127); Seed Funds for Internationalization of Xidian University (2022[17]); the Natural Science Foundation of Shaanxi Province (2022JQ-816); and the scientific research plan projects of the Shaanxi Education Department (21JK0610).

Data Availability Statement: The data are available from the corresponding author upon reasonable request.

Conflicts of Interest: The authors declare no conflict of interest.

References

1. Nie, Z.; Petukhova, A.; Kumacheva, E. Properties and emerging applications of self-assembled structures made from inorganic nanoparticles. *Nat. Nanotechnol.* **2010**, *5*, 15–25. [[CrossRef](#)]
2. Velev, O.D.; Gupta, S. Materials Fabricated by Micro- and Nanoparticle Assembly—The Challenging Path from Science to Engineering. *Adv. Mater.* **2009**, *21*, 1897–1905. [[CrossRef](#)]
3. Li, Y.; Jun-Yan Suen, J.; Prince, E.; Larin, E.M.; Klinkova, A.; Therien-Aubin, H.; Zhu, S.; Yang, B.; Helmy, A.S.; Lavrentovich, O.D.; et al. Colloidal cholesteric liquid crystal in spherical confinement. *Nat. Commun.* **2016**, *7*, 12520. [[CrossRef](#)] [[PubMed](#)]
4. Li, Y.; Khuu, N.; Prince, E.; Alizadehgiashi, M.; Galati, E.; Lavrentovich, O.D.; Kumacheva, E. Nanoparticle-laden droplets of liquid crystals: Interactive morphogenesis and dynamic assembly. *Sci. Adv.* **2019**, *5*, eaav1035. [[CrossRef](#)]
5. Noh, J.; Lagerwall, J.P.F. Topological Defect-Guided Regular Stacking of Focal Conic Domains in Hybrid-Aligned Smectic Liquid Crystal Shells. *Crystals* **2021**, *11*, 913. [[CrossRef](#)]
6. Gao, Y.; Huang, T.F.; Lu, J.G. Template Effect of Multi-Phase Liquid Crystals. *Crystals* **2021**, *11*, 602. [[CrossRef](#)]
7. Kim, S.H.; Park, J.G.; Choi, T.M.; Manoharan, V.N.; Weitz, D.A. Osmotic-pressure-controlled concentration of colloidal particles in thin-shelled capsules. *Nat. Commun.* **2014**, *5*, 3068. [[CrossRef](#)]
8. Nagelberg, S.; Zarzar, L.D.; Nicolas, N.; Subramanian, K.; Kalow, J.A.; Sresht, V.; Blankschtein, D.; Barbastathis, G.; Kreysing, M.; Swager, T.M.; et al. Reconfigurable and responsive droplet-based compound micro-lenses. *Nat. Commun.* **2017**, *8*, 14673. [[CrossRef](#)]
9. Kang, Y.; Xue, R.; Wang, X.; Zhang, T.; Meng, F.; Li, L.; Zhao, W. High-resolution depth imaging with a small-scale SPAD array based on the temporal-spatial filter and intensity image guidance. *Opt. Express* **2022**, *30*, 33994–34011. [[CrossRef](#)]

10. Shipway, A.N.; Katz, E.; Willner, I. Nanoparticle Arrays on Surfaces for Electronic, Optical, and Sensor Applications. *Chemphyschem* **2000**, *1*, 18–52. [[CrossRef](#)]
11. Kim, J.W.; Han, S.H.; Choi, Y.H.; Hamonangan, W.M.; Oh, Y.; Kim, S.H. Recent advances in the microfluidic production of functional microcapsules by multiple-emulsion templating. *Lab Chip* **2022**, *22*, 2259–2291. [[CrossRef](#)]
12. Martino, C.; deMello, A.J. Droplet-based microfluidics for artificial cell generation: A brief review. *Interface Focus* **2016**, *6*, 20160011. [[CrossRef](#)]
13. Paterson, D.A.; Bao, P.; Abou-Saleh, R.H.; Peyman, S.A.; Jones, J.C.; Sandoe, J.A.T.; Evans, S.D.; Gleeson, H.F.; Bushby, R.J. Control of Director Fields in Phospholipid-Coated Liquid Crystal Droplets. *Langmuir* **2020**, *36*, 6436–6446. [[CrossRef](#)] [[PubMed](#)]
14. Bao, P.; Paterson, D.A.; Harrison, P.L.; Miller, K.; Peyman, S.; Jones, J.C.; Sandoe, J.; Evans, S.D.; Bushby, R.J.; Gleeson, H.F. Lipid coated liquid crystal droplets for the on-chip detection of antimicrobial peptides. *Lab Chip* **2019**, *19*, 1082–1089. [[CrossRef](#)]
15. Kolacz, J.; Wei, Q.-H. Self-Localized Liquid Crystal Micro-Droplet Arrays on Chemically Patterned Surfaces. *Crystals* **2022**, *12*, 13. [[CrossRef](#)]
16. Mitov, M.; Portet, C.; Bourgerette, C.; Snoeck, E.; Verelst, M. Long-range structuring of nanoparticles by mimicry of a cholesteric liquid crystal. *Nat. Mater.* **2002**, *1*, 229–231. [[CrossRef](#)] [[PubMed](#)]
17. Peng, C.; Lavrentovich, O.D. Liquid Crystals-Enabled AC Electrokinetics. *Micromachines* **2019**, *10*, 45. [[CrossRef](#)] [[PubMed](#)]
18. Guo, J.K.; Gao, Y.; Ling, J.; Yuan, Y.; Wang, X.; Song, J.K. Laser processing of microdroplet structure of liquid crystal in 3D. *Opt. Express* **2022**, *30*, 26018–26026. [[CrossRef](#)]
19. Li, Y.; Prince, E.; Cho, S.; Salari, A.; Mosaddeghian Golestani, Y.; Lavrentovich, O.D.; Kumacheva, E. Periodic assembly of nanoparticle arrays in disclinations of cholesteric liquid crystals. *Proc. Natl. Acad. Sci. USA* **2017**, *114*, 2137–2142. [[CrossRef](#)]
20. Peng, C.; Turiv, T.; Guo, Y.; Shiyanovskii, S.V.; Wei, Q.H.; Lavrentovich, O.D. Control of colloidal placement by modulated molecular orientation in nematic cells. *Sci. Adv.* **2016**, *2*, e1600932. [[CrossRef](#)]
21. Yoshida, H.; Asakura, K.; Fukuda, J.; Ozaki, M. Three-dimensional positioning and control of colloidal objects utilizing engineered liquid crystalline defect networks. *Nat. Commun.* **2015**, *6*, 7180. [[CrossRef](#)] [[PubMed](#)]
22. Wang, N.; Evans, J.S.; Liu, Q.; Wang, S.; Khoo, I.-C.; He, S. Electrically controllable self-assembly for radial alignment of gold nanorods in liquid crystal droplets. *Opt. Mater. Express* **2015**, *5*, 1065. [[CrossRef](#)]
23. Kim, Y.K.; Senyuk, B.; Lavrentovich, O.D. Molecular reorientation of a nematic liquid crystal by thermal expansion. *Nat. Commun.* **2012**, *3*, 1133. [[CrossRef](#)] [[PubMed](#)]
24. Orlova, T.; Asshoff, S.J.; Yamaguchi, T.; Katsonis, N.; Brasselet, E. Creation and manipulation of topological states in chiral nematic microspheres. *Nat. Commun.* **2015**, *6*, 7603. [[CrossRef](#)]
25. Guo, J.-K.; Vij, J.K.; Song, J.-K. Tunable Transfer of Molecules between Liquid Crystal Microdroplets and Control of Photonic Crystallinity in Isolated Microdroplets. *Adv. Opt. Mater.* **2017**, *5*, 1700119. [[CrossRef](#)]
26. Guo, J.K.; Hong, S.H.; Yoon, H.J.; Babakhanova, G.; Lavrentovich, O.D.; Song, J.K. Laser-Induced Nanodroplet Injection and Reconfigurable Double Emulsions with Designed Inner Structures. *Adv. Sci.* **2019**, *6*, 1900785. [[CrossRef](#)]
27. Guo, J.-K.; Zhao, Z.-J.; Ling, J.-Z.; Yuan, Y.; Wang, X.-R. Laser micro/nanomachining technology for soft matter. *Acta Phys. Sin.* **2022**, *71*, 174203. [[CrossRef](#)]
28. Guo, J.K.; Song, J.K. Three-dimensional reconstruction of topological deformation in chiral nematic microspheres using fluorescence confocal polarizing microscopy. *Opt. Express* **2016**, *24*, 7381–7386. [[CrossRef](#)]
29. Sec, D.; Copar, S.; Zumer, S. Topological zoo of free-standing knots in confined chiral nematic fluids. *Nat. Commun.* **2014**, *5*, 3057. [[CrossRef](#)] [[PubMed](#)]
30. Honaker, L.W.; Sharma, A.; Schanen, A.; Lagerwall, J.P.F. Measuring the Anisotropy in Interfacial Tension of Nematic Liquid Crystals. *Crystals* **2021**, *11*, 687. [[CrossRef](#)]
31. Wang, X.; Kim, Y.K.; Bukusoglu, E.; Zhang, B.; Miller, D.S.; Abbott, N.L. Experimental Insights into the Nanostructure of the Cores of Topological Defects in Liquid Crystals. *Phys. Rev. Lett.* **2016**, *116*, 147801. [[CrossRef](#)] [[PubMed](#)]
32. Trivedi, R.P.; Klevets, I.I.; Senyuk, B.; Lee, T.; Smalyukh, I.I. Reconfigurable interactions and three-dimensional patterning of colloidal particles and defects in lamellar soft media. *Proc. Natl. Acad. Sci. USA* **2012**, *109*, 4744–4749. [[CrossRef](#)] [[PubMed](#)]
33. Posnjak, G.; Copar, S.; Musevic, I. Hidden topological constellations and polyvalent charges in chiral nematic droplets. *Nat. Commun.* **2017**, *8*, 14594. [[CrossRef](#)] [[PubMed](#)]
34. Lopez-Leon, T.; Fernandez-Nieves, A. Drops and shells of liquid crystal. *Colloid Polym. Sci.* **2011**, *289*, 345–359. [[CrossRef](#)]
35. Xu, F.; Crooker, P.P. Chiral nematic droplets with parallel surface anchoring. *Phys. Rev. E* **1997**, *56*, 6853–6860. [[CrossRef](#)]

Disclaimer/Publisher’s Note: The statements, opinions and data contained in all publications are solely those of the individual author(s) and contributor(s) and not of MDPI and/or the editor(s). MDPI and/or the editor(s) disclaim responsibility for any injury to people or property resulting from any ideas, methods, instructions or products referred to in the content.